Int. J. Electrochem. Sci., 14 **(2019)** 3236 – 3244, doi: 10.20964/2019.04.36

International Journal of
ELECTROCHEMICAL
SCIENCE
www.electrochemsci.org

Short Communication

Corrosion of Weathering Steel under Light Illumination and Simulated Atmospheric Conditions

Xiangxiao Qiu[*], *Jifeng Li*, *Zhanqing Liu*

College of Chemistry and Material of WeiNan Normal University, Weinan 714099, China
[*]E-mail: xiangxiaoqiu18@sohu.com

Received: 7 December 2018 / *Accepted:* 16 January 2019 / *Published:* 10 March 2019

Earlier investigations have shown that corrosion products of weathering steel presented photovoltaic effect under illumination. In this study, we explored the influence of chloride ions on this effect and the related corrosion behavior. Open circuit potential, electrochemical impedance spectroscopy and Mott-Schottky plots were recorded on weathering steel surface treated with NaCl after 3 days exposure in simulated atmospheric condition under illumination. For comparison, similar study was also performed on the weathering steel surface without NaCl deposition. There was clearly photoelectrochemical response difference between the samples. It was found that the defects concentration and electric conductivity of the corrosion products were higher due to the chloride ions migration, which was promoted by incorporation of photo-generated holes under illumination. The detailed mechanism was discussed in this study.

Keywords: atmospheric corrosion; chloride ions migration; photovoltaic effect

1. INTRODUCTION

Marine atmospheric corrosion protection is costly [1]. The corrosion behavior of weathering steel exposed to different environments has been explored [2-4]. It has been pointed out that chloride ions migration in the corrosion products plays a main role on the corrosion process in marine atmospheric condition [5-7]. So it is essentially necessary to reveal the interaction between the chloride ions and the corrosion products. Recently, many studies suggest that solar illumination can modify the corrosion products microstructure and composition. Illumination increases the NaCl induced atmospheric corrosion rate of zinc significantly, which can be attributed to the photovoltaic effect of the corrosion products [8]. Illumination obviously accelerates the atmospheric corrosion of Cu. With ozone and NaCl, the accelerating effect of UV is more evident [9]. The corrosion and rust formation behavior of

weathering steel in NaCl solution under illumination is compared with TiO_2 coated weathering steel. The weight loss of the steel in both conditions is increased under UV light in the dipping test, but decreased in the dropping test. It is attributed to the rust formed on the weathering steel behaves similar to the TiO_2 film showing a semiconductor like behavior [10]. However, the influence of corrosion products property on the migration of chloride ions under illumination is still not clear.

The aim of this study is to determine the influence of chloride ions on photovoltaic effect of weathering steel, which were exposed in simulated atmospheric condition under illumination for 3 days. Multiple surface analysis combining with photoelectrochemcial and electrochemical measurements were applied to determine the related photoelectrochemical response and corrosion behavior. The corrosion products electronic structure and electric property were discussed.

2. EXPERIMENTAL

2.1 Sample preparation

All the chemicals used in this study were analytical purity grade reagents purchased from Aladdin and used without further treatment. Weathering steel (WS) is used in this study. Its chemical composition was given in table 1. The size of each sample was 20 mm × 20 mm × 4 mm. Before exposure, each sample was abraded using SiC paper down to 2000 mesh, then cleaned in ethanol, dried with N_2 gas. The sample used for AFM analysis was further polished with diamond paste to 0.25 μm and then cleaned before exposure. All the samples divided into two groups, one group were directly put into exposure apparatus, the other were pre-deposited with NaCl saturated ethanol solution using a microsyringe before exposure. In the present study, the NaCl deposition amount was 4 $\mu g/cm^2$ on the working side of each sample.

Table 1. Chemical composition of the weathering steel (wt.%)

composition	C	Si	Mn	P	S	Cu	Ni	Cr
Weathering steel	0.05	0.30	0.81	0.011	0.005	0.33	0.12	0.70

The simulated atmospheric condition was achieved in a self-assembly exposure chamber, which top lid was fixed with quartz window to supply visible-light transmission. The other part of the chamber was shielded from light. The light source was a 500 W xenon lamp with UV cutoff filter ($\lambda \geq 420$ nm). The humidified air was introduced by the compressed dry air through a couple of humidifier, which contained distilled water with a resistivity of 18MΩ/cm. The exposure was controlled at 95$\pm$3% RH with a temperature of 20$\pm$1℃ and a stable air flow of 50 ml/min along the sample surface. Each exposure was maintained in this condition for 3 days.

2.2 Surface Characterization

The sample surface topography after exposure was observed using atomic force microscopy (AFM, MultiMode 3D SPM System, Bruker Corporation). The probe was the Sb doped n-type Si tip

with a spring constant of 40 N/m and resonant frequency of 300 KHz. All samples were operated in the tapping mode and the scan rate of 1 Hz. The scanning area was 10 μm × 10 μm. The composition of the corrosion products was analyzed with confocal Raman microspectroscopy (CRM). A HORIBAHR-800 system equipped with a 514 nm laser was used. An Olympus ×50Lwd objective was used with a pinhole size of 3 μm. Integration time for each Raman spectrum was 60 s. Scan range was 600-4000 nm. The Raman spectra were generated with LabSpec software.

2.3 Electrochemical measurements

The electrochemical workstation Zahner IM6eX was applied to accomplish the tests. A quartz window which allowed the maximum light transmission was fitted to the front of electrochemical cell then the light passed through the electrolyte to shine the sample surface during the electrochemical tests, which were performed in 1% Na_2SO_4 solution using three-electrode cell system. The exposed sample acted as the working electrode. Its exposed area was 4 cm^2. Platinum filament and saturated calomel electrode (SCE) served as counter electrode and reference electrode, respectively. The light source was a 44 mW tungsten LED lamp operating at wavelength of 420-730 nm. The open circuit potential (OCP) of the rusted WS after 3 days corrosion were recorded with intermittent visible-light on and off. The first stage was in the dark for 30 minutes. Then light illuminates on the sample surface for 30 minutes. Electrochemical impedance spectroscopy (EIS) was performed at OCP, its AC amplitude was 5 mV sinusoidal perturbation and the measurement frequency ranging from 10^4 to 10^{-2} Hz. The commercial software Zsimpwin was used to analysis the experimental data. Mott-Schottky curves were collected at the frequency of 1000 Hz with 5 mV sinusoidal perturbation. The scanning potential was ranging from -0.5 V_{SCE} to -0.2$V_{SCE.}$

3. RESULTS AND DISCUSSION

3.1 Characterization of corrosion products

Figure 1 presents the corroded WS surface topography after 3 days exposure in simulated atmospheric condition under illumination. The surface topography of the specimen without NaCl deposition is evenly distributed. This is clearly different from the specimen with NaCl deposition, which is clustered accompanied by volcano topography. Some studies suggest that the corrosion products protective behavior is strongly rely on its compactness, thickness and density of defects [11-13]. So the corrosion products formed on NaCl deposition specimen cannot prevent the penetration of electrolyte, which may act as transmission channels for oxygen and electrolyte and reduce the corrosion resistance of the metal substrate [11, 14].

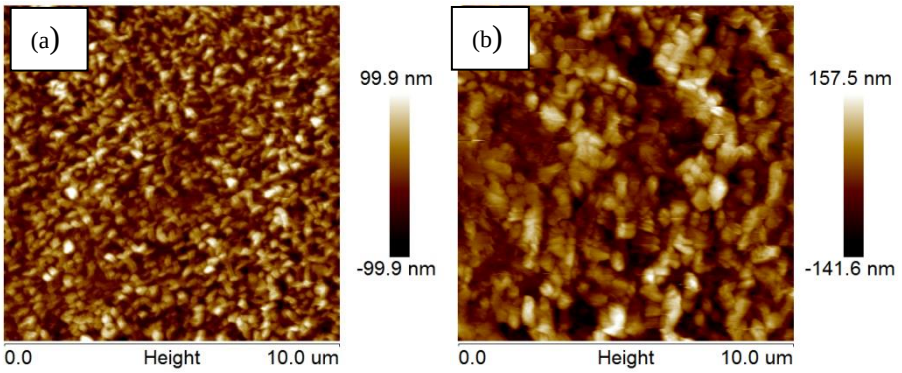

Figure 1. AFM images of WS after 3 days exposure in simulated atmospheric condition (95±3% RH, 20±1℃) under visible-light illumination . (a) Without NaCl deposition (b) with 4μg/cm^2 NaCl deposition

Figure 2 shows the Raman spectra of WS after 3 days exposure in simulated atmospheric condition under illumination. There are peaks at 250 cm^{-1} and 381 cm^{-1}, which are typical of γ-FeOOH. The peaks at 331 cm^{-1}, 542 cm^{-1} and 669 cm^{-1} represents α-Fe_2O_3 [15]. It can be seen that the corrosion products formed on the sample without NaCl deposition are mainly consisted of α-Fe_2O_3. However, the one with NaCl deposition are mainly γ-FeOOH and α-Fe_2O_3. This is consistence with other study that chloride ions can promote the formation of γ-FeOOH [16]. Some studies also observe the dual layered structure formed on weathering steel due to the illumination [17-19]. Furthermore, it has been reported that γ-FeOOH is a strong reducing agent, which can weaken corrosion products resistance property by active cathodic reaction [20].

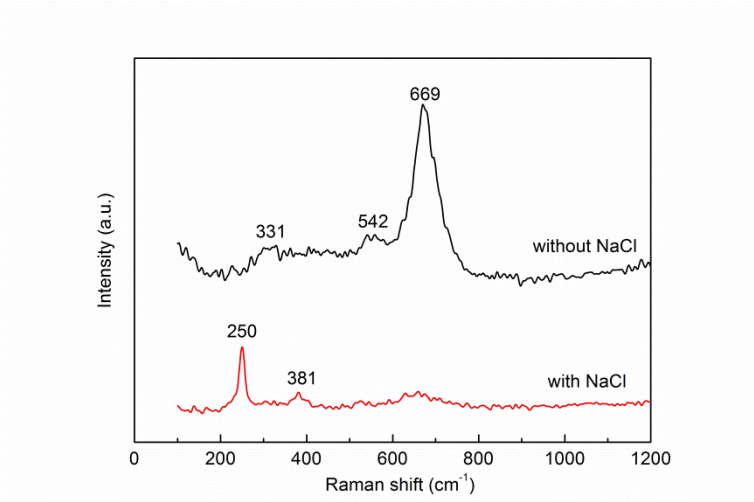

Figure 2. Raman spectra collected on WS surface after 3 days exposure in simulated atmospheric condition (95±3% RH, 20±1℃) under visible-light illumination.WS sample without NaCl deposition denoted as without NaCl and WS sample with 4 μg/cm^2 NaCl deposition denoted as with NaCl in the figure.

3.2 Electrochemical analysis

It's known that the band gap of α-Fe_2O_3 [21-23] and γ-FeOOH [24] are 2~2.4 eV and 2.6 eV, respectively. They can be activated by visible light and generated electron-hole pairs. Photo-voltages is

widely used to analyze the photovoltaic effect of the corrosion products on the metal substrate. This can be achieved by recording the open circuit potential shift under illumination [12]. Figure 3 shows the open potential shift of the corroded WS specimen under intermittent visible-light illumination. The first stage was in the dark for 30 minutes. Then light illuminates on the sample surface for 30 minutes. It can be observed that the potential shift positively under illumination. It has been reported that the photovoltaic effect of corrosion products can promote electrons in the valence band to the conduction band and leave the holes in the valence band under illumination. The photo induced holes generated by the corrosion products could capture the electrons from the anodic dissolution of the metal substrate. This behavior could induce the acceleration of the metal substrate [12, 14].

But the potential can shift negatively much faster on NaCl deposited specimen than without NaCl treated one when the light is turned off. This potential shift is caused by the recombination of electron-hole pairs. It is clear that this recombination process is faster on NaCl pre-deposited sample. This may attribute to the fine conductivity of the corrosion products formed on the sample. In order to get insight on this deduction, electrochemical impedance spectroscopy is recorded.

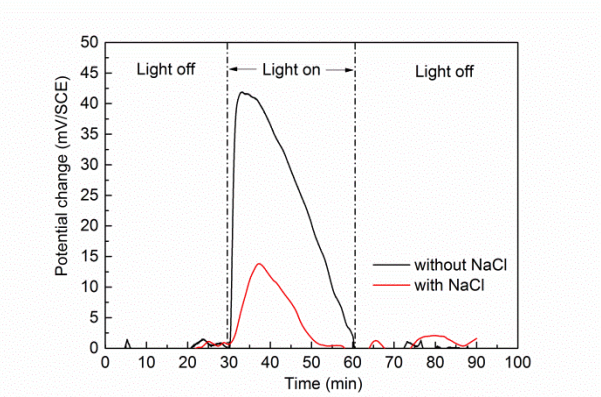

Figure 3. Potential shift collected in 1% Na_2SO_4 solution under intermittent visible-light on and off for WS after 3 days exposure in simulated atmospheric condition (95±3% RH, 20±1℃) under visible-light illumination.WS sample without NaCl deposition denoted as without NaCl and WS sample with 4 μg/cm^2 NaCl deposition denoted as with NaCl in the figure.

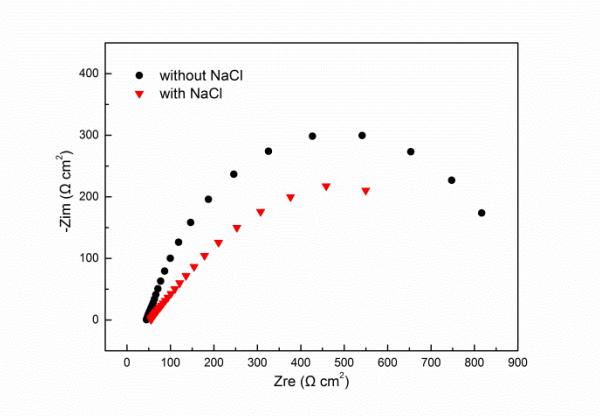

Figure 4. EIS recorded in 1% Na_2SO_4 solution for WS after 3 days exposure in simulated atmospheric condition (95±3% RH, 20±1℃) under visible-light illumination.WS sample without NaCl deposition denoted as without NaCl and WS sample with 4 μg/cm^2 NaCl deposition denoted as with NaCl in the figure.

Figure 4 shows the Nyquist diagrams collected in 1% Na_2SO_4 solution for WS after 3 days exposure in simulated atmospheric condition under illumination. They exhibit two capacitive arcs. Based on the electrochemical process and interface property, the equivalent circuit in figure 5 is built to fit EIS diagrams. The fitting results are listed in table 2. In this equivalent circuit, R_s represents the system resistance of the substrate, solution and electrical cables. R_1 represents the charge transfer resistance of the interface of solution and corroded sample. Q_1 represents the constant phase elements of Helmholtz layer. R_2 and Q_2 represent the resistance and constant phase element of the space charge layer of corrosion products. It can be seen that R_1 and R_2 of the sample with NaCl deposition is smaller than that of without NaCl deposition. So the the charge transfer process and corrosion products resistance are greatly reduced for the WS with NaCl deposition. This observation is agreed with the potential shift findings in figure 3. So the faster electron-hole pairs recombination process presented on the sample is related to its fine conductivity. The interfacial resistance reduction were also found in other studies. They claimed that this behavior can facilitate charge transfer process and lead to the formation of less stable corrosion products [11, 16, 25].

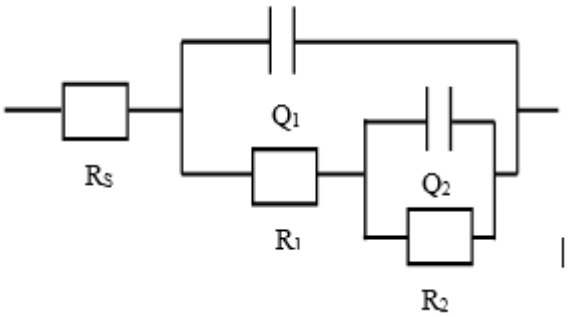

Figure 5. The electrochemical equivalent circuit for EIS fitting.

Table 2. Electrochemical impedance parameters obtained after the fitting of EIS diagrams

condition	R_s	Q_1		R_1	Q_2		R_2
	Ω cm^2	Y_0 /$10^{-4}\Omega^{-1}$cm^{-2}S^n	n_1	Ω cm^2	Y_0 /$10^{-4}\Omega^{-1}$cm^{-2}S^n	n_2	Ω cm^2
Without NaCl deposition	44	6.33	0.74	159.6	0. 61	0.92	830
With NaCl deposition	54	24.24	0.55	89.8	13.68	0.56	634

Figure 6 presents the Mott-Schottky plots collected in 1% Na_2SO_4 solution for WS after 3 days exposure in simulated atmospheric condition under illumination. Based on the linearship between the applied potential and capacitance of the space charge region, the corrosion products display n-type semiconductor property [18]. Earlier studies reveal that n-type corrosion products could induce anodic photocurrent and increase the corrosion rate [14, 26]. The corresponding flat band potential and donor density are calculated based on n-type Mott-Schottky equation. The results are listed in table 3. There is no big difference on the flat-band potential between the samples with or without NaCl deposition. It has

been reported that the difference between the conduction band potential and the flat band potential is very similar for n-type semiconductor [17]. It could be reasonable to consider the flat band potential as its conduction band potential. So it is an indication that the conduction band potential of the two samples is similar. This suggests that the photo-generated electrons reduction property could be similar. However, the donor density is higher for NaCl deposited sample than the other. It indicates that the defects concentration and the electric conductivity of the corrosion products are higher under the effect of chloride ions. It is agree with the EIS interpretation. Similar study also suggests that chloride ions contribute to the increase in the flux of cation vacancy by its absorption into the oxygen vacancy at the corrosion products/electrolyte interface, which could promote Schottky pair formation and cation extraction [13]. The increase in the charge carrier density upon NaCl deposition could also promote the incorporation of photo-generated holes in the corrosion products/electrolyte interface, which decreases the stability of the corrosion products [16-18].

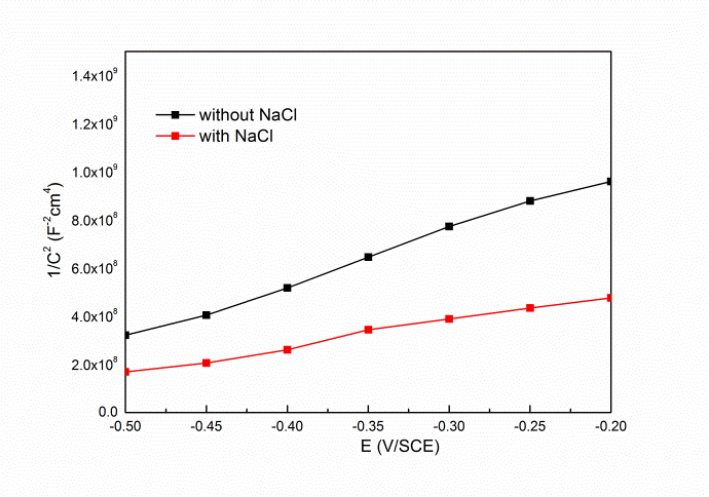

Figure 6. Mott-Schottkey plots recorded in 1% Na_2SO_4 solution for WS after 3 days exposure in simulated atmospheric condition (95±3% RH, 20±1℃) under visible-light illumination.WS sample without NaCl deposition denoted as without NaCl and WS sample with 4 μg/cm^2 NaCl deposition denoted as with NaCl in the figure.

Table 3. Flat band potentials (E_{fb}) and donor density (N_d) estimated from the Mott-Schottkey plots

condition	E_{fb}(V)	N_d(×10^{22} donor)
Without NaCl deposition	-0.47	0.31
With NaCl deposition	-0.43	0.46

The above analyses suggest that NaCl deposition on weathering steel surface, which exposes in simulated atmospheric condition under illumination, can weaken the corrosion products resistance property. This is not only evidenced from the corrosion products topography but also the chemical compositions. It is also attributed to the higher defects concentration and the higher electric conductivity

of the corresponding corrosion products formed. This study confirmed that chloride ions deposition at the corrosion products/electrolyte interface could promote Schottky pair formation and cation extraction by incorporation of the oxygen vacancy and the photo-generated holes. This greatly decreases the stability of the corrosion products.

4. CONCLUSION

This study investigated the influence of chloride ions on photovoltaic effect of weathering steel, which were exposed in simulated atmospheric condition under illumination for 3 days. Based on photoelectrochemical tests and surface analyses, it was found that the corrosion products presented n-type semiconductor property and the corrosion resistance was greatly reduced when the weathering steel surface treated with NaCl. Furthermore, the corresponding corrosion products defects concentration and the photon generated charge migration process were increased. This was because chloride ions deposition at the corrosion products/electrolyte interface could promote Schottky pair formation and cation extraction by incorporation of the oxygen vacancy and the photo-generated holes. This greatly decreased the stability of the corrosion products formed on weathering steel in atmospheric condition under illumination.

ACKNOWLEDGEMENTS
The authors acknowledge the facilities, scientific and technical supports of WeiNan Normal University. We are also grateful to the reviewers for the helpful comments.

References

1. C. Leygraf, T. Graedel, Atmospheric Corrosion, John Wiley & Sons, Inc., New York, 2000.
2. Z. Wang, J. Liu, R. Han, Y. Sun, *Corros. Sci.* 67 (2013) 1.
3. M. Yamashita, T. Mishawa, *Corros. Eng*., 49 (2000) 96.
4. P. Dillmann, F. Mazandier, S. Hoerle, *Corros. Sci*., 46 (2004) 1401.
5. H. E. Townsend, *Corrosion* 57 (2001) 497.
6. Y. Ma, Y. Li, F. Wang, *Corros. Sci*. 51 (2009) 997.
7. P. Qiu, Z. Chen, H. Yang, L. Yang, L. Luo, C. Chen, *Int. J. Electrochem. Sci*., 11(2016) 10498.
8. S. Song, Z. Chen, *J. Electrochem. Soc*., 161 (2014) C288.
9. T. E. Graedel, J. P. Franey, G. W. Kammlott, *Science*, 224 (1984) 599.
10. M. Mahmoud, R. Wang, M. Kato, K. Nakasa. *Script. Mater*., 53 (2005) 1303.
11. S. Deng, H. Lu, D. Li, *Appl. Surf. Sci.,* 462 (2018) 291.
12. L. Song, Z. Chen, *J. Electrochem. Soc*., 162 (2015) C79.
13. H. Jang, H. Kwon, *J. Solid State Electr.* 19(2015) 3427.
14. X. Sun, Z. Chen, J. Li, J. Hou and L. Xu, *Int. J. Electrochem. Sci.,* 13 (2018) 8150
15. L. J. Oblonsky and T. M. Devine, *J. Electrochem. Soc*., 144 (1997) 1252.
16. A. K and M. Kikuchi, *Corros. Sci*., 45 (2003) 2671.
17. J. Ninlachart, K. S. Raja, *ECS Trans.,* 85 (2018)567.
18. L. Song, Z. Y. Chen, B. Hou, *Corros. Sci.*, 93(2015) 191.
19. L. Song , X. Ma, Z. Y. Chen, B. Hou,*Corros. Sci.*, 87(2014) 427.

20. A. Singh, T. Ericsson and L. Hggstrom, *Corros. Sci.*, 25 (1985) 931.
21. R. Spray and K. Choi, *Chem. Mater*., 21 (2009) 3701.
22. H. Uchiyama, M. Yukizawa and H. Kozuka, *J. Phys. Chem*. C, 115 (2011) 7050.
23. B. Klahr and T. W. Hamann, *J. Phys. Chem*. C, 115 (2011) 8393.
24. J. Vequizo and M. Ichimura, *Appl. Phys. Express*, 5 (2013) 125501.
25. A. Burkert, T. Muller, J. Lehmann, J. Mietz, Mater.Corros., 69(2018)20.
26. J. Wielant, V. Goossens, R. Hausbrand and H. Terryn, *Electrochim. Acta*, 52 (2007) 7617.